White light induced photocatalytic activity of sulfur-doped TiO_2 thin films and their potential for antibacterial application

Charles W. Dunnill,[a] Zoie A. Aiken,[b] Andreas Kafizas,[a] Jonathan Pratten,[b] Michael Wilson,[b] David J. Morgan[c] and Ivan P. Parkin*[a]

Received 10th July 2009, Accepted 26th August 2009
First published as an Advance Article on the web 6th October 2009
DOI: 10.1039/b913793a

Sulfur-doped titania thin films were prepared by atmospheric pressure chemical vapour deposition (APCVD) for the first time using titanium tetrachloride, ethyl acetate and carbon disulfide. The films were compared to two industrial self-cleaning products: Activ™ and BIOCLEAN™, and shown to be superior in both photocatalysis and photo-induced superhydrophilicity, two preferential properties of effective self-cleaning coatings. X-Ray diffraction showed the films have the anatase TiO_2 structure. XPS and EDX analysis shows changes in S : Ti ratio with preparative conditions indicating that sulfur has indeed been incorporated into the lattice. S-Doped TiO_2 films were found to be effective agents for killing the bacterium *Escherichia coli* using light sources commonly found in UK hospitals.

Introduction

Titanium dioxide (TiO_2) films have been extensively studied as photocatalysts with recent applications including self-cleaning windows *e.g.* Activ™, BIOCLEAN™ and Sunclean™.[1–3] These self-cleaning windows have a TiO_2 layer on the glass that is 10–50 nm thick and promotes the photocatalytic destruction of organic pollutants as well as forming a photo-induced super-hydrophilic layer.[4–7] The dirt is both loosened by the photo-mineralisation at the interface and then washed off uniformly by rainwater that sheets on the surface due to the hydrophilic properties of the films.[4–7] CVD prepared TiO_2 and doped TiO_2 thin films have been the focus of much of our activity,[5,6,8–17] including improving the activity and application as well as adapting the current technology to other areas such as antibacterial applications.[4,12] One such approach is to shift the band onset from the UV into the visible region of the spectrum to take advantage of the greater abundance of photons at lower energy, as 98% of photons from solar energy have wavelengths >385 nm at the earth's surface.[18] The increase in number of available photons should improve the photocatalytic properties of the film and the availability of a visible light-driven photocatalyst with self-cleaning, or even antimicrobial properties unveils a plethora of potential applications where there is a ready supply of white light and little UV, such as interior household and hospital locations especially with hand-touch surfaces susceptible to bacterial transfer.[4] One approach to making visible light photocatalysts is to dope the TiO_2 structure with anions such as nitrogen[16,17,19–26] or sulfur.[19,27–34] Sulfur-doped TiO_2 has been much studied and put forward as a good photocatalyst, however, it has never been seen in the form of thin films made by APCVD.

Organisms such as *Escherichia coli* and other Enterobacteriaceae are found in the large intestine and are used as indicators of faecal contamination when testing food and food surfaces.[35] This organism is often observed on toilet flush handles, door handles, taps and other areas that are frequently touched by unwashed hands. These, amongst other areas, harbour bacteria and can contribute towards the spread of healthcare-associated infection by acting as reservoirs for infection. Healthcare-associated infections are a significant problem with a yearly cost to the UK taxpayer of around £1bn[36] with organisms such as *Staphylococcus aureus* and *Clostridium difficile* causing significant morbidity and mortality in hospitalised patients. The role of surface bacterial contamination in hospital acquired infection[37] as well as catheter acquired infections has recently been reviewed.[37,38] It has been shown that light-activated antimicrobial coatings are more efficient in killing Gram-positive bacteria such as *S. aureus* than Gram-negative bacteria such as *E. coli*,[39] since Gram-negative bacteria have a more complex cell wall and are more resistant to the radicals formed by photocatalytic reactions. If an antimicrobial coating was effective against *E. coli*, it would serve as a good marker for antimicrobial action against other organisms such as methicillin-resistant *S. aureus* (MRSA). Photo-activated antimicrobial surfaces therefore represent a fundamental weapon in the fight against healthcare-associated infections alongside the traditional methods such as good hand hygiene and regular cleaning.

Here we report the production of a series of white light-driven photocatalytic films of sulfur-doped TiO_2 (S-TiO_2) produced utilising a simple methodology, consistent with technology and techniques currently employed in the float glass industry. The system has been investigated for the trends associated with sulfur content, utilising the temperature of the volatile sulfur precursor as a measure of the sulfur contribution in the deposition mixture. Carbon disulfide was used in these preparations as it has advantages industrially over other reagents such as hydrogen sulfide as it is considerably less toxic,[40–42] and easier to handle as a liquid and there are also twice the available sulfur atoms per molecule compared to H_2S. The series of films produced have

[a]*Centre for Materials Research, Department of Chemistry, University College London, 20 Gordon Street, London, UK WC1H 0AJ. E-mail: I.P.Parkin@ucl.ac.uk*
[b]*UCL Eastman Dental Institute, University College London, 256 Gray's Inn Road, London, UK WC1X 8LD*
[c]*Cardiff Catalysis Institute, School of Chemistry, Cardiff University, Main Building, Park Place, Cardiff, UK CF10 3AT*

been compared to two of the current industry leading products for self-cleaning glass: Pilkington Activ™ and Saint-Gobain BIOCLEAN™. We show that the S-doped films are effective photocatalysts, and that one film type in particular is effective in killing *E. coli* with the white light commonly used in UK hospitals. This work, to our knowledge, constitutes the first study of S-doped titania prepared by simple CVD methods to kill bacteria. S-Doped TiO_2 powders formed by sol–gel have been observed to have antibacterial properties on the Gram-positive bacteria *Micrococcus lylae*.[43]

Experimental

Synthesis

CVD preparations were carried out using a custom built, horizontal, cold-walled APCVD quartz deposition chamber. The deposition chamber consisted of a 360 mm long quartz tube, 100 mm diameter and with a graphite reactor-bed containing three cartridge heaters (Whatman) on which the glass substrates were positioned. A steel sheet was used to limit the volume of the reactor, giving the reacting gasses approximately 7 mm of space above the glass substrate.

A preheated carrier gas (nitrogen, BOC Gases, Guildford, UK 99%) was supplied from a cylinder, bubbled through the reservoirs and passed into the heated mixing chambers prior to reaching the glass substrate in the deposition chamber. At each stage the temperature and flow of the nitrogen were independently controlled.

The depositions were carried out on the SiO_2 surface of slides of standard float glass from NSG Pilkington[44] of dimensions 220 × 85 × 4 mm (length × width × thickness) coated on one side with a barrier layer of SiO_2 to prevent ion diffusion from the glass to the film. The glass was washed prior to insertion into the APCVD reactor using sequential washings of water, acetone, petroleum ether (60–80 °C) and propan-2-ol giving a clean and smear free finish.

In all preparations discussed the glass substrates were heated at 10 °C min^{-1} from room temperature to 500 °C and allowed to equilibrate for >45 min, prior to the deposition reactions. The precursors used were titanium tetrachloride ($TiCl_4$) (Aldrich) as the titanium source, ethyl acetate (EtAc) (BOC Gases, 99%) as the oxygen source and carbon disulfide (CS_2) (Alfa Aesar, 99.9%) as the sulfur source. The nitrogen carrier gas for the $TiCl_4$ and EtAc was preheated to ~150 °C with a flow rate of 0.5 L min^{-1}. The bubblers were heated to 70 and 40 °C, respectively, to give a molar mass flow ratio of 1 : 2. These reactants were premixed in a single mixing chamber at 250 °C with an additional flow of 6 L min^{-1} carrier gas (N_2) preheated to 150 °C. The sulfur doping was achieved using a preheated carrier gas at 60 °C flowing at 0.3 L min^{-1} through the carbon disulfide reservoir whose temperature was controlled using a water bath containing 50 : 50 H_2O : ethylene glycol (0–10 °C). The carbon disulfide was introduced to the $TiCl_4$ and EtAc mixture just before contact with the glass substrate at a temperature of 100 °C and an additional flow of 1 L min^{-1}, as shown in the schematic in Fig. 1.

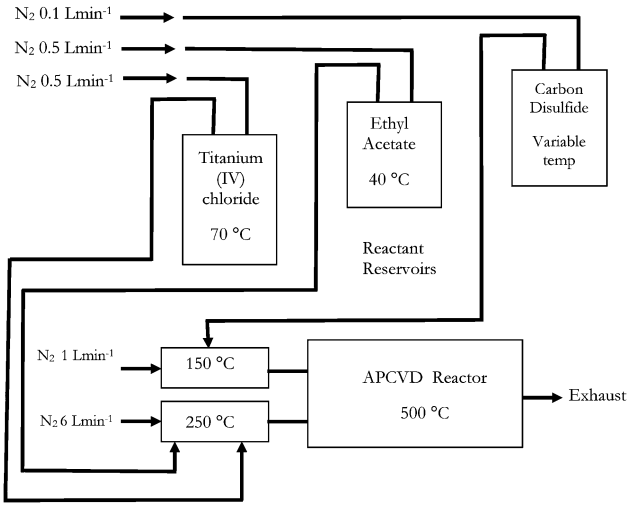

Fig. 1 Schematic of the gas lines and reactant reservoirs used in the preparations discussed. The temperature and flow rate of the $TiCl_4$ and EtAc reservoirs lead to a ratio of ~1 : 2.5 $TiCl_4$: EtAc in the gas phase which is desirable for the growth of anatase films under the conditions of the reactor.

The mass flow rate of the carbon disulfide was calculated from the volatility data for carbon disulfide and is given in Table 1 which also shows the sample preparation conditions and the sample references used throughout.

Characterisation

X-Ray diffraction was achieved using a Bruker-Axs D8 (GADDS) diffractometer, utilising a large 2D area detector and a Cu X-ray source, monochromated (Kα1 and Kα2) fitted with a Gobble mirror. The instrumental setup allowed 34° in both θ and ω with a 0.01° resolution and 3–4 mm^2 of sample surface illuminated at any one time. Multiple Debye–Scherrer cones were recorded simultaneously by the area detector with two

Table 1 Table showing the sample names and the experimental conditions for the thin films of S-doped TiO_2 formed from the APCVD of $TiCl_4$, ethyl acetate and carbon disulfide at 500 °C. The sample names are those used in the figures with the relative information given in the legends. Samples **A**, **B** and **C** refer to the two industry standards Activ™ and BIOCLEAN™ and a sample of the untreated glass, respectively

Sample	Temperature of CS_2 reservoir/°C	Molar mass flow of CS_2/mmol min^{-1}	Approx gas phase mass flow ratios $TiCl_4$: EtAc : CS_2	Deposition time/s
D (TiO_2)	N/A	N/A	1 : 2.5 : 0	30
E (S-TiO_2)	0	2.5	1 : 2.5 : 0.9	30
F (S-TiO_2)	5	3.3	1 : 2.5 : 1.2	30
G (S-TiO_2)	10	4.4	1 : 2.5 : 1.6	30

sections covering the 65 °2θ range. The Debye–Scherrer cones were integrated along ω to produce standard 1D diffraction patterns of °2θ against intensity. Scan data were collected for 800 s to give sufficiently resolved peaks for indexing. Raman spectra were achieved using a Renishaw inVia Raman microscope, and UV-vis, transmission and reflectance measurements were achieved using a Perkin Elmer λ950. Scanning electron microscopy was performed using secondary electron imaging on a JEOL 6301 field emission instrument with Oxford instruments EDX spectrometer attached. X-Ray photoelectron spectroscopy (XPS) was performed at Cardiff University using a Kratos Axis Ultra-DLD photoelectron spectrometer using monochromatic Al-K_α radiation. Survey spectra were collected at a pass energy of 160 eV, whilst narrow scans acquired at a pass energy of 40 eV, charge neutralisation of the samples was achieved using the Kratos immersion lens neutralisation system. The data were analysed using CasaXPS™ software and calibrated to the C(1s) signal at 284.7 eV, attributed to adventitious carbon.

Functional testing

In these experiments the photoactivity of the films was quantified using three methods: firstly the effect on the contact angle between the film and water, secondly the destruction of the redox dye 2,6-dichloroindophenol (DCIP) and thirdly the destruction of a stearic acid overlayer. Both white light experiments were carried out using white light from a source commonly found in UK hospitals (General Electric 28 W Biax 2D compact fluorescent lamp). The spectral distribution chart is given in Fig. 2.

The water droplet contact angle was assessed by storing the samples in a dark clean cupboard for >72 h and applying a 5 µl drop of deionised water to the surface. The water droplet diameter was measured and from that the contact angle was calculated. The samples were dried and subjected to UV-light illumination to fully clean the surface before the water droplet test was performed. The DCIP dye mixture was prepared in a similar fashion to intelligent ink, as formulated by Mills *et al.*[45] The ink comprises 3 g of a 1.5 wt% aqueous solution of HEC polymer, 0.7 g of glycerol and 9 mg of the redox dye, DCIP, and was applied to the surface of the film using a refillable marker pen as three uniform spots and allowed to dry. The photocatalytic

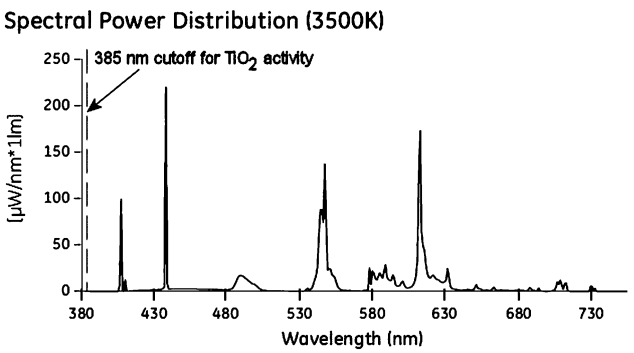

Fig. 2 Spectral power distribution diagram for the lamp used in the visible light photocatalysis measurements,[53] marked with the cut-off for the activity of TiO_2, *i.e.* only photons of higher energy than 385 nm can activate TiO_2. The nearest emission line is at 410 nm. This light source is in common use in UK hospitals.

reduction on the film was monitored by a digital photographic method between illuminations under the white light source. Digital TIF images (200 ppi) were recorded using an Epson Perfection 1200 Photo Scanner and Windows Scanner Software. Red-green-blue values from digital images were acquired using custom-made software, entitled RGB Extractor©, written using Visual Basic 6.0 software. This software is freely available.[46] Red-green-blue values extracted were averages of 100 colour data pixels (10 × 10 squares) centred on each of the three spots. The outcome is a series of values from 0 to 255 indicating the redness of the blue dye on a white background at different time intervals (the *R* value tends to 255 as the spot disappears). This test allows a quick and semi-quantitative measure of the photocatalytic properties of the films in an easily comparable way.

Once evaluated semi-quantitatively by DCIP, the samples were tested by monitoring the destruction of a stearic acid overlayer. In general stearic acid measurements involve applying the stearic acid to the surface and monitoring its destruction using the IR peaks that correspond to the C–H stretches in the stearic acid molecules. Stearic acid absorbs at: 2958 cm^{-1} (C–H stretch CH_3), 2923 cm^{-1} (symmetric C–H stretch CH_2), and 2853 cm^{-1} (asymmetric C–H stretch CH_2). The first peak is generally ignored as it is of low intensity and the other two peaks are integrated to give an approximate concentration of stearic acid on the surface. 1 cm^{-1} in the integrated area corresponds to approximately 9.7×10^{15} molecules cm^{-2}.[47] The rate of decay can then be approximated and compared as C_x/C_0 readings, where C_0 is the initial concentration of stearic acid present and C_x is the concentration at any time x.

The samples for stearic acid testing were prepared in duplicate as sheets of ~30 × 30 mm with as uniform a thin film as possible. These sheets were irradiated in a light box under UV (254 nm) radiation to ensure that the surfaces were clean and active and attached to an IR sample holder consisting of an aluminium sheet with a circular hole in its centre. The samples were then stored in a clean dark drawer for >72 h to ensure that no activation by UV-light was remaining. A 0.01 M solution of stearic acid in methanol was then applied drop-wise by Pasteur pipette to the centre of the hole and allowed to evaporate, leaving the characteristic white smear of stearic acid. Once dried the C_0 reading was taken and the samples placed in a white light box and irradiated for a period of 24 h. Readings were taken at 24 h intervals for the remainder of the experiment, ~200 h.

For the microbiology testing, *E. coli* ATCC 25922 was stored at −80 °C in 10% glycerol and maintained by weekly subculture onto 5% Columbia blood agar plates (Oxoid Ltd., Basingstoke, UK). A single colony was inoculated into 20 mL nutrient broth (Oxoid Ltd., Basingstoke, UK) and incubated for 18 h at 37 °C in a rotating incubator (Sanyo BV, Loughborough, UK, 200 rpm). 1 mL of the overnight culture was centrifuged at 12 000 rpm, and the pellet was re-suspended in 1 mL of phosphate-buffered saline. Approximately 300 µL of this suspension were added to 10 mL phosphate-buffered saline to achieve an optical density of 0.05 on a spectrophotometer at a wavelength of 600 nm (GE Healthcare, Buckinghamshire, UK), which equated to approximately 10^7 colony forming units per mL. The suspension was diluted and aliquoted onto MacConkey agar plates and aerobic colony counts calculated after 48 h incubation at 37 °C to estimate the bacterial load of the original inoculum.

During the microbiology testing two irradiation steps were carried out: a pre-activation by white light (A) and an illumination by white light (L). All films were handled exactly the same within their set parameters and incubated in the same incubator. The thin film surfaces were either exposed to both irradiation steps (A+ L+) or as controls, the activation step and not the illumination (A+ L−), the illumination step and not the activation (A− L+) or incubated in the dark throughout, with no light exposure (A− L−). Two bacterial counts were produced for each exposure condition and the experimental procedure was performed in triplicate to demonstrate reproducibility.

The white light source used was the same as in the other photocatalysis measurements (General Electric 28 W Biax 2D compact fluorescent lamp), emitting an average light intensity of 5950 lux at 20 cm from the source. This was used as it is a typical light source supplied to many UK hospitals (a typical hospital pathology lab has 5000 lux; operating theatres 10 000–100 000 lux and hospital corridors 50–100 lux[48]). After the initial irradiation period, 50 μL of the prepared bacterial suspension (approximately 5.0×10^5 cfu cm^{-3}) were added to each of the thin film surfaces before returning to the light source for a further 24 h. The bacterial droplet was sampled for 20 s with a pre-moistened cotton-tipped swab, using a uniform, standardised method (the surface was sampled in three directions whilst rotating the head to ensure maximum absorbency) before re-suspending the swab in 1 mL phosphate-buffered saline. After a 2 min vortex, dilutions of 10^{-1}, 10^{-2} and 10^{-3} were plated out onto MacConkey plates, in duplicate and incubated for 48 h at 37 °C. Aerobic colony counts were determined and the results compared to the controls.

The viable count data were subjected to statistical analysis using the Mann–Whitney test in the SPSS program (version 16.0, SPSS Inc., Chicago, IL, USA). The films exposed to both irradiation steps (A+ L+) were compared to the three sets of controls (A− L+, A+ L− and A− L−) to determine the effect of activation, and light exposure.

In all the functional testing the white light source was positioned about 20–25 cm from the samples giving a highly intense luminosity supply. It should be noted that in a hospital environment the luminosity will largely depend on the location. General corridors and wards containing door handles, bathrooms containing taps and flush handles will have a lower luminosity (50–100 lux) and the photocatalysts will therefore work slower than in the experimental setup. In an operating theatre where there is a significant need for higher sterility the lighting sources are far more intense (10–100 klux). The light levels used in our experiments closely match the conditions used for a hospital pathology laboratory (5000 lux).

Results and discussion

Synthesis and characterisation

S-Doped titania films were prepared by the APCVD reaction of $TiCl_4$, ethyl acetate and carbon disulfide at a substrate temperature of 500 °C and a deposition time of 30 s. Films with varied sulfur content were formed using different mass flow rates of carbon disulfide (2.5, 3.3 and 4.4 mmol min^{-1}). TiO_2 is generally difficult to dope with non-metal elements especially larger ones such as sulfur[27] with the so far successful routes being to heat a titania film to high temperature under H_2S[33] and to oxidise TiS substrates,[19,34] both of these routes have disadvantages compared to the use of CS_2 during the TiO_2 synthesis. Other synthetic procedures in the literature to form S-doped titania are for powders rather than thin films and tend to use some form of sol–gel method for their synthesis.[19,28,30,31,43] The use of CVD to form doped TiO_2 is much more prevalent in the N-doped system that has been published previously.[16,17] One advantage of using APCVD to form S-TiO_2 is that the technology is entirely compatible with the industrial processes for the formation of self-cleaning glass and the incorporation of a sulfur source into the industrial process would be easy for coating glass as it comes off the float line. This is far superior to post-treating using a sol–gel synthesis. This is, however, only one application for this sort of technology.

The S-doped films described herein appeared almost colourless, but with a slight yellow tinge and transparent with uniform thickness and were well adhered to the glass substrate. They were unable to be removed using Scotch tape and were resistant to scratching by fingernails, pencil (HB) and a steel scalpel. The films were able to be scratched using a diamond pencil. In all cases the film was inspected by eye post-treatment. Sample names are given in Table 1.

X-Ray diffraction data (Fig. 3) of the films show peaks that match in position to those expected for anatase TiO_2. No rutile peaks were observed. It appears that the crystallinity of the films decreases slightly with higher sulfur content. This decrease in crystallinity is known to happen in other doped systems of TiO_2 such as nitrogen-doped TiO_2, especially at high concentrations.[48,49] Highly crystalline systems are found to be better photocatalysts than their poorly crystalline analogues so high doping concentrations would likely result in poor performance for photocatalysts.[15] Preferred orientation along the 211 direction of the crystal structure is observed in the XRD pattern indicating a high level of preferential growth of the crystallites within the film as indicated by the platelet like appearance in the SEM images (Fig. 4). The exact position of the reflections shifts slightly

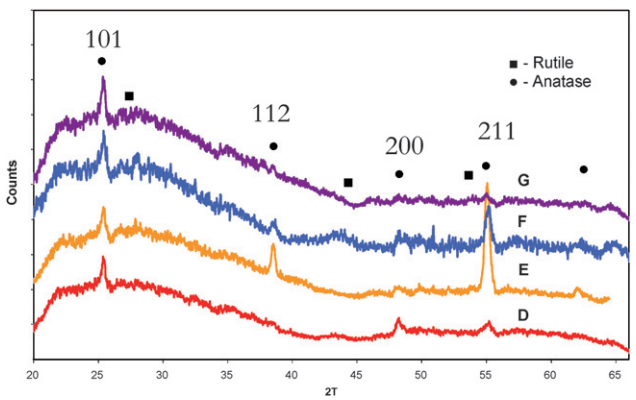

Fig. 3 XRD patterns for the thin films of S-doped TiO_2 formed from APCVD of $TiCl_4$, ethyl acetate and carbon disulfide at 500 °C, showing the peaks that correspond to peak positions for anatase (●) and rutile (■) structures within the different S-doped TiO_2 films. Preferred orientation is observed along the 211 miller indices. Samples **D**, **E**, **F** and **G** were prepared with a molar mass flow of 0, 2.5, 3.3 and 4.4 mmol min^{-1}, respectively, for the carbon disulfide and 30 s deposition times.

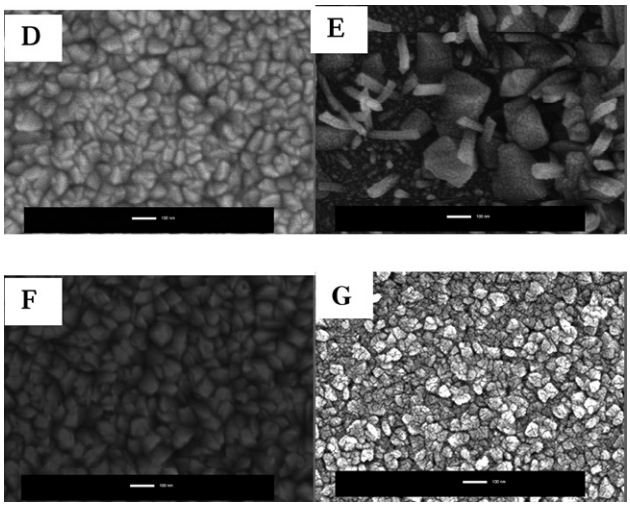

Fig. 4 SEM micrographs of the films of S-doped TiO_2 formed from APCVD of $TiCl_4$, ethyl acetate and carbon disulfide at 500 °C showing the nanoparticulate nature of the thin films and the difference in size of the particulates in each case. Samples **D**, **E**, **F** and **G** were prepared with a molar mass flow of 0, 2.5, 3.3 and 4.4 mmol min^{-1}, respectively, of the carbon disulfide and 30 s deposition times. All images taken at 100 000× magnification. Scale bar represents 100 nm.

as sulfur is incorporated indicating a minimal expansion of the lattice—however, this was difficult to accurately quantify.

Raman spectroscopy (Fig. 5) shows a clear presence of anatase with no rutile contribution in any of the samples. At 500 °C the synthesis would be expected to prepare the anatase structure rather than rutile which tends to be seen at higher deposition temperatures.[8] Sample **E** appears to be very slightly shifted to higher wave numbers though samples **F** and **G** remain unchanged with respect to anatase, sample **D**. This shift in **E** could indicate a change in structure for example oxygen vacancies as a result of sulfur incorporation.[50]

It has been noted that in powders there is a relationship between the rutile and anatase compositions *vs.* the sulfur concentration. Low dopant concentrations of sulfur gave the rutile polymorph and high dopant concentrations gave anatase.[51] In contrast, the thin films show low sulfur concentrations clearly seen to be present with the anatase polymorph.

Scanning electron microscopy (Fig. 4) shows that the films are made up of nanoparticulates of varying shape and size. The largest particles are observed in sample **E** with the lowest concentration of sulfur along with needle-like objects. There is very little difference in morphology between samples **D**, **F** and **G** though there is a significant difference between these three and sample **E**. EDX showed the presence of sulfur within the structure but was below the level of accurate quantification. However, sulfur was observed at 0.08–0.19 at.% for samples **E–G**. In this respect the samples are similar to those observed in the literature, only the nanoparticles here are adhered to the substrate as a thin film rather than held as a nanoparticulate suspension. Whilst lowering the surface area the films are significantly easier to handle if being used as a heterogeneous catalyst.

UV-visible transmission (Fig. 6) data show that all films are >70% transparent in the visible region of the spectrum allowing their use in windows and similar applications. All films were seen to be 200–300 nm thick using the Swanepoel method based on the interference pulses seen in the UV-visible spectra.[52] A clear shift of the band onset in the direction of the visible region of the spectrum is observed for the S-doped samples. Further each of the three S-doped films shows an enhancement in band onset position when compared to either the pure TiO_2 or the two industrial products (again pure TiO_2). The order of the shift from left to right is: sample **C**, **B**, **A**, **D**, **E**, **G**, and **F**. Sample **F** prepared with a 1 : 1.2 ratio of $TiCl_4$: CS_2 exhibits the highest shift in band onset, compared to untreated glass.

The position of the band onset was estimated using Tauc plots (Fig. 7). The plots were extrapolated along their lengths to the *x* axis from the steepest parts of the curve to give the estimated band onset position. A similar trend to that found from the transmission data was observed. The estimated positions for the

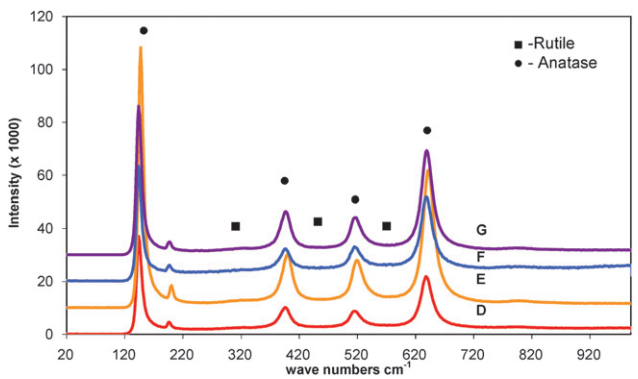

Fig. 5 Raman spectroscopy of the thin films of S-doped TiO_2 formed from APCVD of $TiCl_4$, ethyl acetate and carbon disulfide at 500 °C, showing no evidence for the rutile structure and a clear indication that the anatase structure of TiO_2 is present in all samples. ■ and ● indicate positions of expected rutile and anatase peaks, respectively.[57] Samples **D**, **E**, **F** and **G** were prepared with a molar mass flow of 0, 2.5, 3.3 and 4.4 mmol min^{-1}, respectively, for the carbon disulfide and 30 s deposition times.

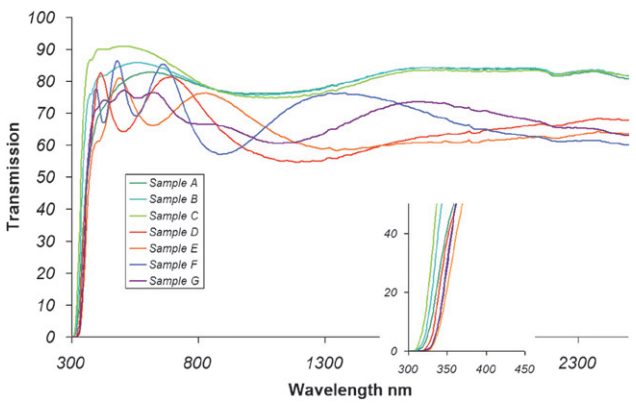

Fig. 6 Transmission UV-visible IR data between 2500 and 300 nm for all the thin films including the S-doped TiO_2; inset shows the expansion of the vertical regions. For clarity purposes the order of the band onsets, indicated by the shift in vertical position from left to right is: **C**, **B**, **A**, **D**, **G**, **F**, and **E**. **A** = Activ™, **B** = BIOCLEAN™, **C** = glass. The S-doped films were formed from APCVD of $TiCl_4$, ethyl acetate and CS_2 prepared at 500 °C and a deposition time of 30 S. Samples **D**, **E**, **F** and **G** were prepared with a molar mass flow of 0, 2.5, 3.3 and 4.4 mmol min^{-1}, respectively, for the carbon disulfide and 30 s deposition times.

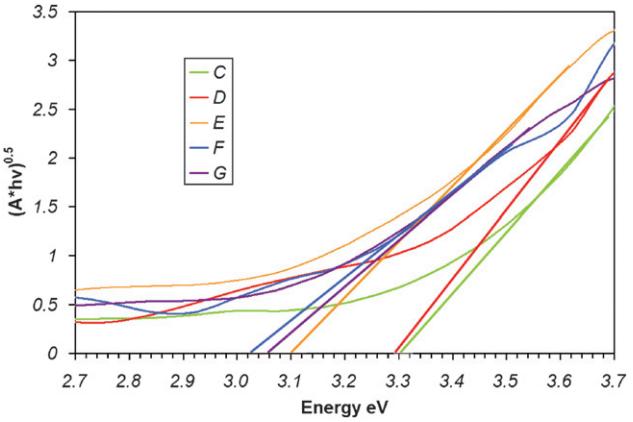

Fig. 7 Tauc plots estimating the band onset for the different S-doped TiO_2 films showing the variation in band onset with mass flow of carbon disulfide. **A** = Activ™, **B** = BIOCLEAN™, **C** = glass. The S-doped films were formed from APCVD of $TiCl_4$, ethyl acetate and CS_2 prepared at 500 °C and a deposition time of 30 s. Samples **D**, **E**, **F** and **G** were prepared with a molar mass flow of 0, 2.5, 3.3 and 4.4 mmol min^{-1}, respectively, for the carbon disulfide and 30 s deposition times. The positions of the extrapolated lines on the *x* axis are given to the nearest 0.05 eV.

band onset are: **D** and **C**: 3.3 eV, **E**: 3.1 eV, **G** and **F**: 3.05 eV. Both samples **F** and **G** exhibit a band onset that is just within the visible light range, *i.e.* <3.1 eV. Sample **F** also has a feature in the Tauc plot that would correspond to a band onset at higher energy. Previous work on sol–gel powders from supercritical fluid based syntheses of S-doped TiO_2 gave a band onset of 2.7 eV at 1.8% S-dopant.[50]

High resolution XPS clearly showed the presence of sulfur within the lattice indicating that at the surface at least there was sulfur incorporation into the structure. The S 2p ionisation was observed at high energy 169.1 eV indicating that it is likely bound in the form of S^{6+}. Sulfur 2p ionisation usually appears in the range 162–171 eV depending on the oxidation state and position of bonding atoms.[28] Peaks due to a Ti–S bond are expected to occur at the lower end of the range, ~163 eV.[28] This suggests that the sulfur has entered the lattice as a cation, possibly replacing the Ti^{4+} ions, similar to the observation by Ohno *et al.*[32] rather than the O^{2-} ions as described by Umebayashi *et al.*[19] Ohno *et al.* observed S^{6+} at 167.6 eV in S-doped TiO_2. The sulfur has been oxidised during the deposition as it has changed from S^{2-} to S^{6+}. There was a trend in Ti : S ratio indicating that the higher the sulfur content in the reaction mixture, the higher the sulfur content in the films. The Ti : S ratios were 1 : 0, 1 : 0.02, 1 : 0.08 and 1 : 0.18, respectively, from sample **D** to sample **G**. These values are very small and close to the resolution of the X-ray photoelectron spectrometer leading to inaccuracy with their exact value though they do show that sulfur is present in small quantities. It is clear that there is a gradient in sulfur content that is dependent on the concentration of CS_2.

Functional testing—hydrophilicity and photocatalysis

Contact angle measurements (Table 2) show marked changes of the water contact angles between sample **D** (TiO_2) and the S-doped samples (**E**, **F** and **G**) when irradiated under UV (365 nm) light for a period of 24 h. All S-doped samples exhibit superhydrophilicity (contact angle <10°) which is a beneficial effect for self-cleaning windows.

Table 2 Table to show the contact angle measurements for the different films of S-doped TiO_2 formed from APCVD of $TiCl_4$, ethyl acetate and carbon disulfide at 500 °C and the untreated glass substrate. The samples were stored in a dark container for 4 days prior to testing for the "Before" measurement. The "After" measurements occurred after 24 h activation by 365 nm radiation. Samples **D**, **E**, **F** and **G** were prepared with a molar mass flow of 0, 2.5, 3.3 and 4.4 mmol min^{-1}, respectively, of the carbon disulfide and 30 s deposition times

Sample	Before irradiation/°	After irradiation/°
C	70	70
D	52	16
E	80	7
F	68	7
G	76	6

The redox dye 2,6-dichloroindophenol (DCIP) was used as a rapid colorimetric test for the presence of photocatalytic functional properties. The results show that the S-doped films are active under the white light source used.[53] In these experiments all S-doped films showed enhanced photocatalytic activity when compared to sample **D**, the pure titania film. The best performers were, however, the lower concentrations of sulfur content with **E** and **F** performing significantly better than the other two samples. Samples **E** and **F** showed a change of 52 RGB units in the 9 h while samples **D** and **G** showed a change of only 28 RGB units.

The thin films were then analysed for their potential to photo-oxidise stearic acid molecules on the surface (Fig. 8). In these tests the best performance was observed from sample **F** with some activity observed by sample **G**. No destruction of stearic acid was observed on the plain glass, Activ™ and BIOCLEAN™ or sample **D**. Interestingly sample **E** which showed a high activity with the DCIP testing showed no activity on these experiments and sample **G** which was not very active using DCIP showed activity using stearic acid outlining the importance of using a range of methods to assess the photocatalytic properties of the films.

The results from the microbiology studies (Fig. 9) showed that only one sample, **F**, had any inherent antimicrobial properties

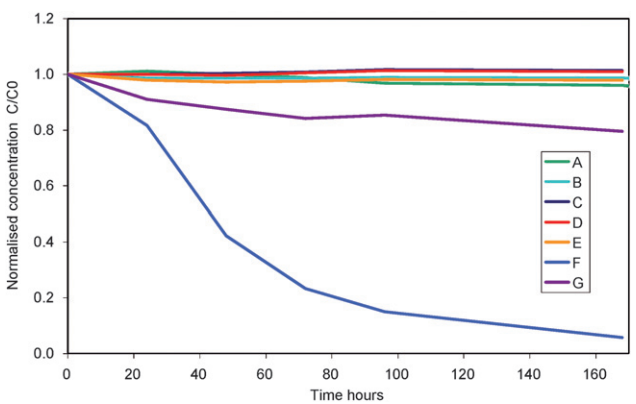

Fig. 8 Results showing the normalised destruction of stearic acid with respect to time. Samples **D**, **E**, **F** and **G** were prepared with a molar mass flow of 0, 2.5, 3.3 and 4.4 mmol min^{-1}, respectively, for the carbon disulfide and 30 s deposition times.

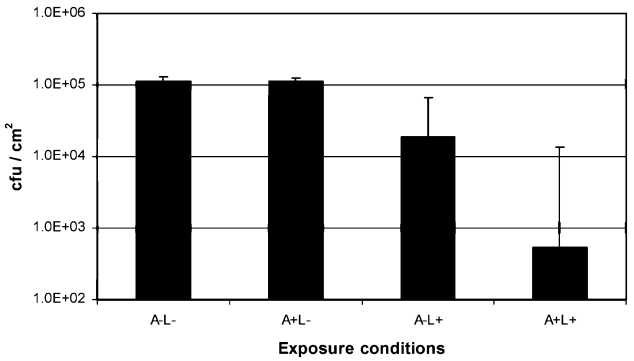

Fig. 9 Survival of *E. coli* on sample **F**. The thin films were exposed to two 24 h light doses (A+ L+) or as controls exposed to the illumination step and not the activation step (A− L+), the activation step and not the illumination step (A+ L−) or incubated in the dark throughout, with no light exposure (A− L−). A 50 μL aliquot of *E. coli* was added after the activation stage. Bars indicate median values ($n = 3$) and error bars indicate the interquartile range.

when exposed to white light. A statistically significant kill of 99.5% (or 2.3 $\log_{10}$ reduction) of *E. coli* was observed on the thin films exposed to both white light doses ($p < 0.01$). The 24 h white light activation step prior to the application of the *E. coli* suspensions did not significantly enhance the activity of the thin films and there was no statistical difference between the activated and non-activated groups *i.e.* A+ L+ *vs.* A− L+ ($p = 0.44$) and A+ L− and A− L− ($p = 1.00$). This thin film corresponds with the best sample from both the DCIP and the stearic acid measurements indicating that both stearic acid and DCIP combined show a good gauge of whether a thin film is likely to exhibit antimicrobial properties.

This is the first report to our knowledge of light-activated antimicrobial properties of S-doped thin films. Furthermore statistically significant kill was obtained using a common hospital white light source and a common hospital bacterium. This kill was noted only for one particular dopant concentration but was reproducible for three different **F** samples with experiments repeated three times. It has been shown that Gram-negative bacteria are less susceptible to photo-induced destruction than Gram-positive bacteria.[39] It is therefore likely that these surfaces will perform better on bacteria such as *M. lylae* as studied by Yu *et al.* making direct comparison impossible between our thin films and the S-doped powders reported.[43]

The use of visible light to kill bacteria has also been reported for N-doped TiO_2,[54] C + N-doped[55] TiO_2 and C-doped TiO_2.[56] Conveniently all of the studies used *E. coli* as a model system, however, direct comparison of effectiveness is difficult between all experiments because of different cfu concentrations, light intensities, as well as different methods of presenting the data and doing the microbiology testing. However, the best S-doped film reported here has at least comparable light-activated antimicrobial properties.

Conclusions

The incorporation of sulfur into TiO_2 thin films has been shown to enhance the photocatalytic properties, especially in the case of sample **F**. This could result from the red shifting of the band onset towards and in the case of sample **F** into the visible region of the spectrum or from the incorporation of sulfur atoms in the lattice disrupting the recombination of electron and hole pairs for enough time to promote migration to the surface and the formation of radical species on the surface of the films, allowing for self-cleaning films to function better under hospital lighting conditions. The S-doped TiO_2 films show possibilities for applications in antimicrobial fields under hospital lighting conditions by killing 99.5% of *E. coli*, a Gram-negative bacterium in 24 h of irradiation. The concentration of the sulfur atoms is critical with low levels of dopants preferable. In all cases the sulfur dopants have been <0.19 at.% incorporation, by XPS.

Acknowledgements

The authors thank the EPSRC for financial support. IPP thanks the Royal Society Wolfson trust for a merit award. DJM also thanks the EPSRC for the Access to Research Equipment initiative (grant number EP/F019823/1).

References

1 http://www.pilkington.com/applications/products2006/english/downloads/byproduct/selfcleaning/default.htm.
2 http://www.selfcleaningglass.com.
3 http://www.suncleanglass.com.
4 A. Mills and S. Le Hunte, *J. Photochem. Photobiol., A*, 1997, **108**, 1–35.
5 I. P. Parkin and R. G. Palgrave, *J. Mater. Chem.*, 2005, **15**, 1689–1695.
6 A. Mills, N. Elliott, I. P. Parkin, S. O'Neill and R. J. H. Clark, *J. Photochem. Photobiol., A*, 2002, **151**, 171–179.
7 A. Mills and M. McFarlane, *Catal. Today*, 2007, **129**, 22–28.
8 G. Hyett, M. Green and I. P. Parkin, *J. Am. Chem. Soc.*, 2006, **128**, 12147–12155.
9 G. Hyett, R. Binions and I. P. Parkin, *Chem. Vap. Deposition*, 2007, **13**, 675–679.
10 A. Kafizas, S. Kellici, J. A. Darr and I. P. Parkin, *J. Photochem. Photobiol., A*, 2009, **204**, 183–190.
11 G. Hyett, M. A. Green and I. P. Parkin, *J. Photochem. Photobiol., A*, 2009, **203**, 199–203.
12 K. Page, R. G. Palgrave, I. P. Parkin, M. Wilson, S. L. P. Savin and A. V. Chadwick, *J. Mater. Chem.*, 2007, **17**, 95–104.
13 A. Mills, A. Lepre, N. Elliott, S. Bhopal, I. P. Parkin and S. A. O'Neill, *J. Photochem. Photobiol., A*, 2003, **160**, 213–224.
14 A. Mills, G. Hill, S. Bhopal, I. P. Parkin and S. A. O'Neill, *J. Photochem. Photobiol., A*, 2003, **160**, 185–194.
15 S. A. O'Neill, I. P. Parkin, R. J. H. Clark, A. Mills and N. Elliott, *J. Mater. Chem.*, 2003, **13**, 56–60.
16 C. Dunnill and I. P. Parkin, *Chem. Vap. Deposition*, 2009, **15**, 171–174.
17 C. W. H. Dunnill, Z. A. Aiken, J. Pratten, M. Wilson, D. J. Morgan and I. P. Parkin, *J. Photochem. Photobiol., A*, 2009, **207**, 244–253.
18 W. Curdt, P. Brekke, U. Feldman, K. Wilhelm, B. N. Dwivedi, U. Schuhle and P. Lemaire, *AIP Conf. Proc.*, 2001, **598**, 45.
19 T. Umebayashi, T. Yamaki, H. Itoh and K. Asai, *Appl. Phys. Lett.*, 2002, **81**, 454–456.
20 G. Hyett, M. A. Green and I. P. Parkin, *J. Am. Chem. Soc.*, 2007, **129**, 15541–15548.
21 A. V. Emeline, V. N. Kuznetsov, V. K. Rybchuk and N. Serpone, *Int. J. Photoenergy*, 2008, **2008**, 258394.
22 Y. Guo, X.-W. Zhang, W.-H. Weng and G.-R. Han, *Thin Solid Films*, 2007, **515**, 7117–7121.
23 Y. Guo, X.-W. Zhang and G.-R. Han, *Mater. Sci. Eng., B*, 2006, **135**, 83–87.
24 H. M. Yates, M. G. Nolan, D. W. Sheel and M. E. Pemble, *J. Photochem. Photobiol., A*, 2006, **179**, 213–223.

25 C. Di Valentin, E. Finazzi, G. Pacchioni, A. Selloni, S. Livraghi, M. C. Paganini and E. Giamello, *Chem. Phys.*, 2007, **339**, 44–56.
26 M. Gartner, P. Osiceanu, M. Anastasescu, T. Stoica, T. F. Stoica, C. Trapalis, T. Giannakopoulou, N. Todorova and A. Lagoyannis, *Thin Solid Films*, 2008, **516**, 8184–8189.
27 Q. Zhang, J. Wang, S. Yin, T. Sato and F. Saito, *J. Am. Ceram. Soc.*, 2004, **87**, 1161–1163.
28 L. Randeniya, A. Murphy and I. Plumb, *J. Mater. Sci.*, 2008, **43**, 1389–1399.
29 Y. Wang, J. Li, P. Peng, T. Lu and L. Wang, *Appl. Surf. Sci.*, 2008, **254**, 5276–5280.
30 D. B. Hamal and K. J. Klabunde, *J. Colloid Interface Sci.*, 2007, **311**, 514–522.
31 L. G. Hongyan Liu, *J. Am. Ceram. Soc.*, 2004, **87**, 1582–1584.
32 T. Ohno, T. Mitsui and M. Matsumura, *Chem. Lett.*, 2003, **32**, 364–365.
33 K. Borowiec, *Scand. J. Metall.*, 1991, **20**, 198–204.
34 S. Yamamoto, A. Takeyama and M. Yoshikawa, *Nucl. Instrum. Methods Phys. Res., Sect. B*, 2006, **242**, 377–379.
35 *Health Protection Agency—Commission of the European Communities*, 2005.
36 *Department of Health: Winning Ways: Working Together to Reduce Healthcare Associated Infection in England*, 2003.
37 K. Page, M. Wilson and I. P. Parkin, *J. Mater. Chem.*, 2009, **19**, 3819–3831.
38 S. Noimark, C. Dunnill, M. Wilson and I. P. Parkin, *Chem. Soc. Rev.*, 2009, DOI: 10.1016/j.jphotochem.2009.07.024.
39 V. Decraene, J. Pratten and M. Wilson, *Appl. Environ. Microbiol.*, 2006, **72**, 4436–4439.
40 http://msds.chem.ox.ac.uk/CA/carbon_disulfide.html.
41 http://msds.chem.ox.ac.uk/HY/hydrogen_sulfide.html.
42 O. Glemser, H. Sauer, *Handbook of Preparative Inorganic Chemistry*, ed. G. Brauer, 1965, Academic Press, New York, p. 932, .
43 J. C. Yu, W. Ho, J. Yu, H. Yip, P. K. Wong and J. Zhao, *Environ. Sci. Technol.*, 2005, **39**, 1175–1179.
44 http://www.pilkington.com.
45 A. Mills, M. McGrady, J. Hepburn and J. Wang, *Int. J. Photoenergy*, 2008, **2008**, 504945.
46 http://www.chem.ucl.ac.uk/people/ipparkin/documents/RGB_Extractor_2_1.zip.
47 A. Mills and J. Wang, *J. Photochem. Photobiol., A*, 2006, **182**, 181–186.
48 BSEN 12464-1:2002; ISBN 0580411281F. D. Duminica, F. Maury and R. Hausbrand, *Surf. Coat. Technol.*, 2007, **201**, 9349–9353.
49 T. Okato, T. Sakano and M. Obara, *Phys. Rev. B: Condens. Matter*, 2005, **72**, 115124.
50 H. Li, X. Zhang, Y. Huo and J. Zhu, *Environ. Sci. Technol.*, 2007, **41**, 4410–4414.
51 X. Wu, D. Wu and X. Liu, *Appl. Phys. A: Mater. Sci. Process.*, 2009, **97**, 243–348.
52 R. Swanepoel, *J. Phys. E: Sci. Instrum.*, 1983, **16**, 1214.
53 http://www.gelighting.com/eu/resources/literature_library/prod_tech_pub/downloads/biax2d_datasheet_0506.pdf.
54 M.-S. Wong, W.-C. Chu, D.-S. Sun, H.-S. Huang, J.-H. Chen, P.-J. Tsai, N.-T. Lin, M.-S. Yu, S.-F. Hsu, S.-L. Wang and H.-H. Chang, *Appl. Environ. Microbiol.*, 2006, **72**, 6111–6116.
55 Q. Li, R. Xie, Y. W. Li, E. A. Mintz and J. K. Shang, *Environ. Sci. Technol.*, 2007, **41**, 5050–5056.
56 D. Mitoraj, A. Janczyk, M. Strus, H. Kisch, G. Stochel, P. B. Heczko and W. Macyk, *Photochem. Photobiol. Sci.*, 2007, **6**, 642–648.
57 L. Burgio and R. J. H. Clark, *Spectrochim. Acta, Part A*, 2001, **57**, 1491–1521.